On Geophysical Property Modelling of Sea Ice: Microstructure and Salinity

Sönke Maus

Geophysical Institute, University of Bergen, email: sonke.maus@gfi.uib.no

Abstract

Geophysical sea ice properties are often defined with respect to a certain scale. The salinity of sea ice is a property that influences the role of sea ice in systems of many different scales. Proper modelling of the salinity's dependence on growth conditions, and the related change in other sea ice properties, requires the detailed knowledge of the distribution of salt within the microstructure of sea ice. Here a simple framework is presented of how sea ice salinity is related to its basic microstructure scales and how the latter quantitatively vary with growth conditions. Different modes of convective stability near the ice-water interface and in the bottom fraction of the ice are key processes in this respect. The analysis shows further how salt entrapment in sea ice and the vertical extent of the near-interface skeletal layer depend on the seawater salinity. It offers a perspective toward improved understanding of the difference in geophysical properties of ice grown from sea- and brackish water.

1 Introduction

It is well known that sea ice contains saline brine in pores and fluid inclusions, while lake ice does not[1,2,3,4]. The corresponding microstructure and salt content of sea ice are important in natural systems where sea ice geophysics is of interest. The dependence of the mechanical properties of sea ice on its microstructure and salinity is relevant in engineering applications, like traffic-ability and offshore technology in polar regions[5,6,7,8]. Biologists focus on the ecosystem of sea ice which is strongly linked to the presence and mobility of brine in pores[9,10]. The relation between microstructure and dielectric sea ice properties is important for remote sensing applications[11]. Last but not least does the role of sea ice in the climate system involve a large number of geophysical mechanisms where the sea ice microstructure and salinity are relevant[12,13,14,15].

Concise geophysical modelling of sea ice requires models of its macroscopic properties on the scale of interest. Common to most of the mentioned research fields is that the role of sea ice depends fundamentally on the entrapment and rejection process of salt during its growth and decay, which in turn has to be related to its microscopic structure. However, a basic theory of the formation and evolution of the sea ice microstructure, and the involved salinity entrapment, is still outstanding. That sea ice contains, depending on age and growth conditions, 5 to 50 % of the seawater salinity from which is formed, has long been known[16?,12,3]. However, observations of how the salt content of sea ice varies with ice thickness and external forcing are still limited. For example, a large number of empirical relations have been proposed for the variation of sea ice salinity with ice thickness. Three frequently cited relations are compared in Figure 1 with two sets of observations from the Arctic and Antarctic. Several other salinity growth sequences are shown in Figure 2. It illustrates the lack of a unique relationship between bulk salinity and thickness for thin ice. To properly describe salt rejection during early growth of ice one apparently has to take the large variability in growth conditions into account.

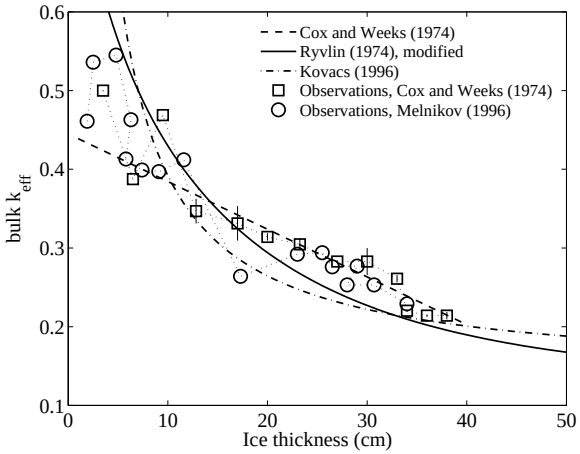

Figure 1: *Growth sequences of bulk* $\overline{k_{eff}}$ *of Arctic*[17] *and Antarctic*[18] *ice, shown with three suggested bulk relations*[17,19,20]*. Adopted from ref.*[21]*.*

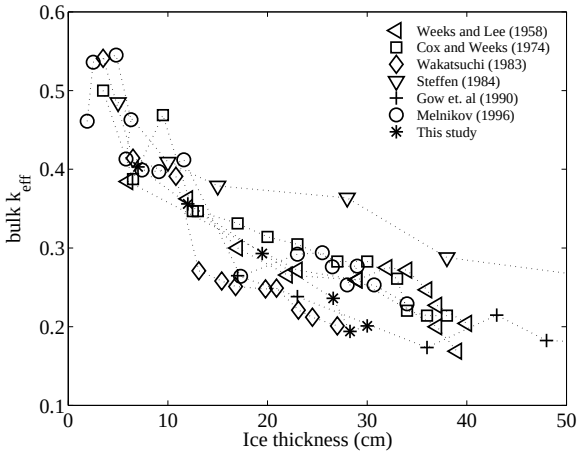

Figure 2: *Growth sequences of bulk* $\overline{k_{eff}}$ *(ratio of ice and seawater bulk salinities) of thin ice from several studies, to be compared with figure 1. Adopted from ref.*[21]*.*

The salinities of thicker ice are, as long the ice is growing and not warming too much, less variable. The rule of thumb - that first-year ice contains one-sixth of the salinity of underlying water - was first suggested by Moss[22] and has been verified in many later studies[? 12,3]. Also most suggested empirical relations[17,19,20] converge, for 1 to 2 meter thick ice, to values similar to this rule. However, the physical processes that imply this constancy have not been clarified so far. A concise explanation has necessarily to consider the entrapment and mobility of brine, and thus to involve a model of the sea ice microstructure's dependence on growth conditions. Intuitively one can argue that a quasi-constant ice salinity is related to less variable growth conditions and the thermal inertia of thick ice, a useful concept that may be sufficient in a number of applications. When it comes to more detailed predictions of macroscopic properties of thic ice, or when its desalination during the summer season is of interest, a theoretical framework of the structural evolution also becomes relevant for thick ice.

In the present paper a simple model of salt/brine entrapment due to the evolution of the sea ice micro-structure is outlined. The basic idea is to (i) predict the sea ice microstructure at the interface in dependence on growth conditions and (ii) formulate the microstructural change with decreasing temperature and increasing distance from the interface. It will be seen how the scales of interest depend on different modes of convection near the interface. Finally several examples will be given to illustrate how one may proceed with geophysical property modelling of sea ice on the basis of this model.

2 Concept of salt entrapment

In principle, due to the generally 2-3 orders of magnitude slower diffusion of solute compared to heat, the desalination of growing sea ice needs to be associated with convective fluid motion. In the absence of external turbulence the convection may be thought to have its driving force in the salinity gradients set up by the rejection of salt from pure ice. However, parametrisations of sea ice desalination employed to date do not account for this process

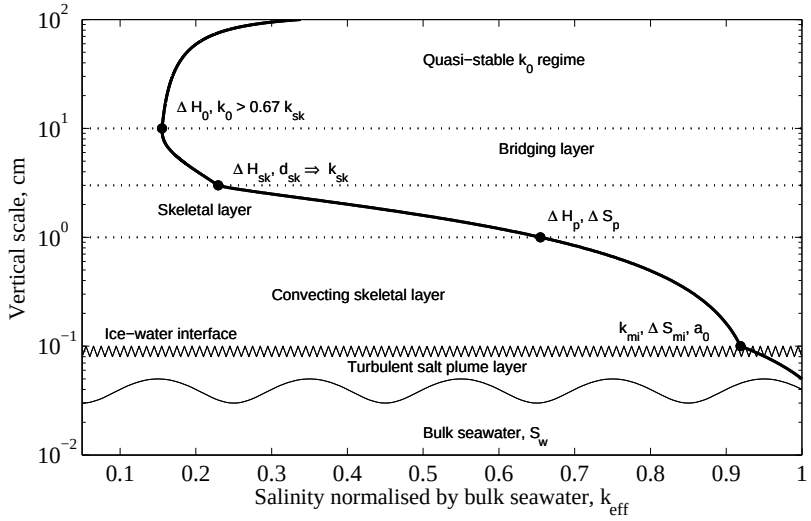

Figure 3: *Conceptual desalination of sea ice near the ice-water-interface, showing different regimes and boundary layers on a logarithmic scale: Rigorous convection takes place in the lower skeletal layer up to ΔH_p, while bridging between plates starts near ΔH_{sk}. At the distance ΔH_0 from the interface a quasi-stable salinity is reached. The local bulk salinity is normalised($k_{eff} = S_i/S_w$). Morphological changes are sketched in figure 4.*

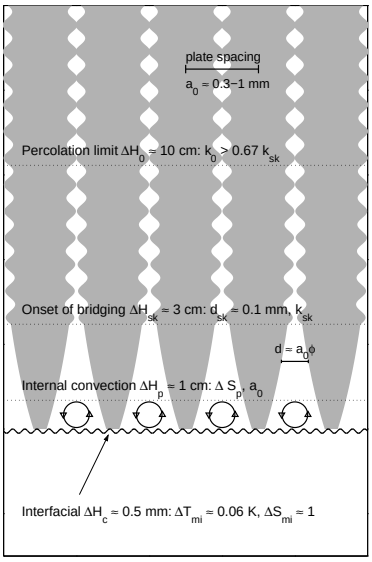

Figure 4: *Typical morphology and porosity near the interface of growing sea ice. View is normal to the plates whose spacing scale is exaggerated by a factor of 100.*

of *free convection*. The most widely used approach[23,24,25,3,26,27,28,29] is based on a forced convection model once suggested for growth of rotating crystals in metallurgy[30]. It is often reported in the form

$$k_{eff} = \frac{k_*}{k_* + (1 - k_*) exp\left(-\frac{V}{D_s}\delta_b\right)}, \tag{1}$$

with solute diffusion coefficient D_s, growth velocity V and a boundary layer scale δ_b. According to (1) the ratio of ice to seawater salinities, $k_{eff} = S_i/S_w$, increases with growth velocity from its slow growth limit k_*. A detailed discussion of why this approach has only very limited applicability for natural ice growth may be found in ref.[21], with main aspects summarised as follows. Both k_* and δ_b in (1) need to be found by a fit to observations. However, these main parameters of (1), a velocity independent k_* and a constant stagnant boundary layer of width δ_b, may, if at all, describe solute redistribution for planar interfaces. They do neither have an empirical nor a physical basis when considering cellular ice growth. Moreover does the assumption of molecular salt transport in a thin interfacial boundary layer of high salinity contrast create a misleading picture of the desalination process (and a physically meaningless quantity δ_b). The parametric form (1) may fit data in a very limited velocity regime yet is inconsistent with the main physical principles of sea ice desalination which are: (i) salt entrapment within a cellular microstructure, (ii) variation of the cellular structure with growth conditions and (iii) delayed desalination by solute-driven internal convection.

Structural modelling of salt entrapment

The present approach, developed in detail in ref.[21], considers salt entrapment in sea ice as a step-wise process on the basis of several boundary layers dominated by different physical processes as sketched in figures 3 and 4. Sea ice grows with a cellular interface consisting of vertically oriented plates between which the entrapped brine is sandwiched. This *plate spacing* a_0 is the fundamental structural parameter of salt entrapment. It depends on growth velocity and the solute transport in a thin turbulent interfacial boundary layer of thickness ΔH_c. The salt flux through the latter is linked to the constitutional supercooling ΔT_{mi} (and the corresponding salinity step ΔS_{mi}) necessary to keep the interface cellular. The plate spacing further controls the near-bottom permeability and thus the salinity increase ΔS_p that may build up internally within the ice before the interlamellar brine convects. This defines an internal boundary layer of thickness ΔH_p measured upward from the ice-water interface. It is further assumed that intermittent convection within ΔH_p will also limit the brine salinity increase up to ΔH_{sk}, marking the upper level of the lamellar skeletal layer. At this level, given by a critical brine layer of width d_{sk} and a brine volume $\phi_{sk} \approx d_{sk}/a_0$, bridging between the ice plates strongly decreases the permeability, finally rendering the flow resistance so large that the salinity gradient can not longer drive fluid motion. From two-dimensional percolation theory this is expected near $\phi_0/\phi_{sk} \approx 0.676$, e.g. ref.[31]. In summary, desalination is assumed to be driven by intermittent exchange of brine with salinity $(S_w + \Delta S_{mi} + \Delta S_p)$ against seawater, S_w, and further freezing of the latter. Percolation then sets an upper bound on the possible desalination between ΔH_{sk} and ΔH_0, and a lower bound $k_0 \approx 0.676 k_{sk}$.

In terms of this model concept the salt entrapment at the level ΔH_{sk} is given by

$$k_{sk} = r_\rho r_{gra} \frac{d_{sk}}{a_0} \left(1 + \frac{\Delta S_{mi} + \Delta S_p}{S_w}\right), \tag{2}$$

and depends on the structural length scales d_{sk} and a_0 and the salinity increase ΔS_p and ΔS_{mi} in the boundary layers. The factors r_ρ and r_{gra} are corrections slightly larger than one relate to the ice-brine density difference and the finite extent of crystals[21]. The challenge is to find physically consistent solutions for the structural parameters and the salinity change in the boundary layers. The stable salinity is then obtained from $k_0 \approx 0.676 k_{sk}$.

Plate spacing and morphological stability

That a robust prediction of the plate spacing may be obtained in terms of a macroscopic approach of classical linear stability theory for a planar interface[32,33] has been outlined in some detail[21,34]. Fundamental to this theory is the criterion of *constitutional supercooling*: (i) solute released at a freezing interface depresses the freezing point, (ii) as solute diffuses much slower than heat there will be a solutal boundary layer where the water is supercooled, and (iii) an initial perturbation of a planar freezing interface thus enters a supercooled regime may eventually grow further - a cellular interface develops. Neglecting the effect of surface tension (curvature depression of the freezing point), temperature gradients due to superheat in the water, and the details of the temperature gradient near the interface, this supercooling must exceed $\Delta T_{mi} \approx (L_v D_s)/(k_i + k_w)$, where k_i and k_w are thermal conductivities of ice and water, D_s the solute diffusivity and L_v the volumetric heat of fusion. At marginal stability, corresponding to this least value of supercooling, the plate spacing may be expected to be

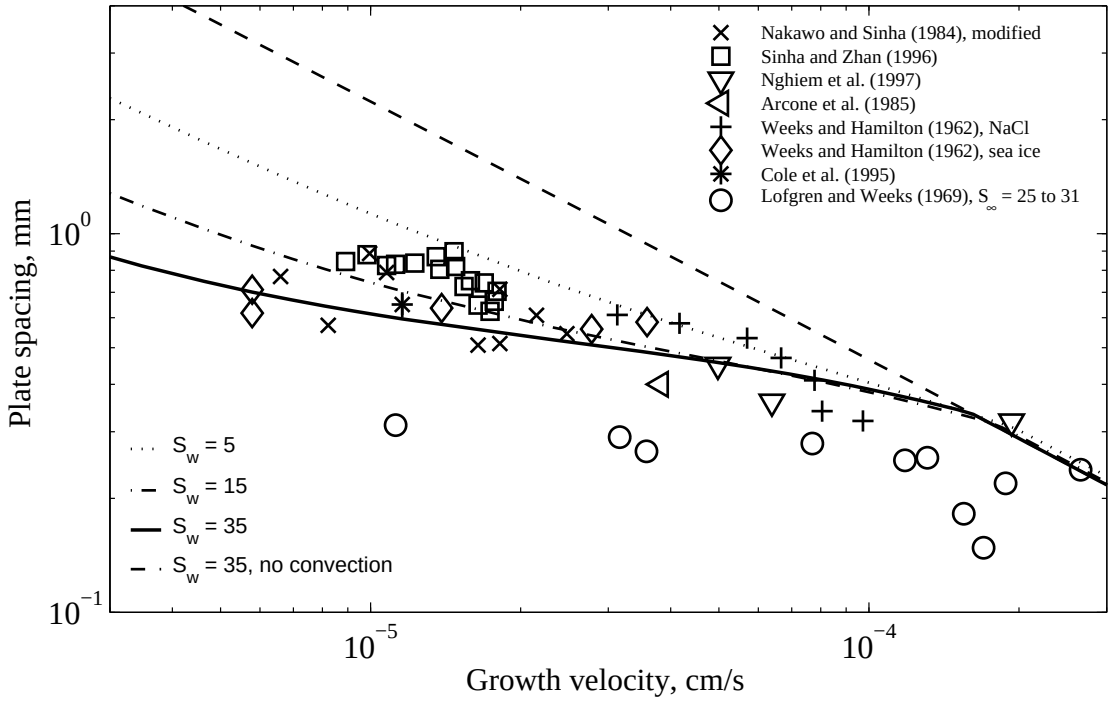

Figure 5: *Predicted plate spacings without (dashed curve) and including the convection model (solid) along with observations of sea ice and laboratory-grown NaCl ice. From ref.[21], with predictions for $S_w = 15$ and 5 added.*

given by

$$a_0 \approx 2\pi 2^{1/3} \left(\frac{D_s}{V}\right)^{2/3} \left(\frac{\Gamma}{\Delta T_{mi} k}\right)^{1/3}, \tag{3}$$

where $\Gamma = T_m \gamma_{sl}/L_v$ is the Gibbs-Thompson parameter based on the solid liquid interfacial energy γ_{sl} and absolute melting temperature T_m (in Kelvin). $k(S_w)$ is the minimum effective interfacial k at which the interface is sufficiently supercooled. Neglecting again curvature effects the latter is approximately given by $k \approx (1 - \Delta T_{mi}/(mS_w))^{-1}$, where $m = dT_f/dS$ is a linearised local freezing temperature slope. The critical k thus decreases with S_w.

Equation (3) is valid as long the solute transport is by diffusion only and the width of the diffusive boundary layer is given as $\approx D_s/V$. However, above a critical growth velocity V_{cr} convection sets in and controls the boundary layer scale[a]. The dependence of a_0 on V becomes then weaker than $a_0 \sim V^{-2/3}$ in the diffusive regime. Figure 5 shows good agreement between theoretical and observed plate spacings. The significantly lower plate spacing in laboratory experiments of ref.[35] (circles) are likely explainable by strong thermal convection in the container[21]. Rather little field observations were available to the author to validate the predicted increase in a_0 at lower water salinities: plate spacings of $0.7 - 0.8$ mm reported for rapidly growing young ice in the Bay of Bothnia[36] exceed those of young Arctic Sea ice by a similar factor as in the theoretical prediction. This salinity dependence is also qualitatively consistent with the laboratory data from ref.[35].

[a]Note that the appropriate boundary layer scale $D_s/V_{cr} \approx 0.4$ mm is much smaller than values proposed on the basis of equation (1)

Skeletal layer convection

The critical brine salinity increase within the skeletal layer is computed from stability theory for freezing porous media, frequently called theory of 'mushy layers'[37,38,39], by evaluating the Rayleigh number

$$Ra_p = \frac{\beta \Delta S_p(z) g K(z) \Delta H_p}{\nu(z)\kappa_b(z)} > Ra_{pc} \tag{4}$$

based on salinity increase ΔS_p across the layer height $\Delta H_p = z$, with haline contraction coefficient β, gravity acceleration g, the kinematic viscosity ν and thermal diffusivity κ_b of brine. The permeability K is a measure of the cross-section of pores through which fluid flows. For an ensemble of infinite vertical brine layers of width d and spacing a_0 it takes the simple form

$$K = \frac{d^2\phi}{12} = \frac{\phi^3 a_0^2}{12}. \tag{5}$$

The critical Rayleigh number Ra_{pc} above which convection begins depends on boundary conditions, vertical and horizontal anisotropy and heterogeneity, e.g.[40,41,42,43]. Moreover, when K varies by more than an order of magnitude, as in the sea ice skeletal layer, it is still not clear how an effective K should be computed[43]. In an earlier work the author[21] suggested a local Rayleigh Number criterion, on the basis of local properties at each z-level, yet based on $\Delta H_p(z) = z$ and the brine salinity increase measured upward from the freezing interface ($z = 0$). An analysis of two experimental studies[24,44] then indicated a critical $Ra_{pc} \approx 6$. Here a physically more reliable criterion, the harmonic mean value of K/ν averaged upward from the interface, was employed to reanalyse the results. This yielded average values of $Ra_{pc} \approx 11$ and 14 for $S_w > 35$ and the respective datasets. The critical Ra_{pc} for $10 < S_w < 20$ however was considerably lower, in the range 2 to 4. No observations to evaluate Ra_{pc} at lower salinity are available. However, as argued below, a value of $Ra_{pc} \approx 0.25$ might be an appropriate limit. In the following calculations $Ra_{pc} = 11, 2$ and 0.25 are assumed for seawater salinities of $35, 15$ and 5.

Bridging transition and percolation

The maximum ΔH_p and ΔS_p obtained from the critical Ra_{pc} and equation (4) yield the maximum salinity increase within the skeletal layer. ΔS_p then enters equation (2) from which k_{sk} is determined. The remaining property to be determined in (2) is the critical width at which bridging of ice plates starts and transforms the basically lamellar structure into brine patches and pore networks. So far limited observations have located it 2 to 4 cm from the interface[45], consistent with the typical skeletal layer thickness, see figure 9 below. However, to date there are no direct observations of the critical brine layer width at which bridging starts between ice plates. A value of 0.07 mm noted as the 'minimum layer width before splitting of brine layers'[46] may eventually be interpreted as a lower bound. Some observations of 'pinch-off' of brine pockets indicate its onset when the brine layers have shrunk to a width of $\approx 0.05 - 0.10$mm[47,48]. A discussion of more recent microstructure statistics indicates that a plausible value is between $0.08 < d_{sk} < 0.12$ mm[21]. A concise theoretical explanation is still outstanding[b].

[b]The minimisation of surface energy, as frequently suggested[46,49,50], may be rejected because the brine layers are minimum energy surfaces[21].

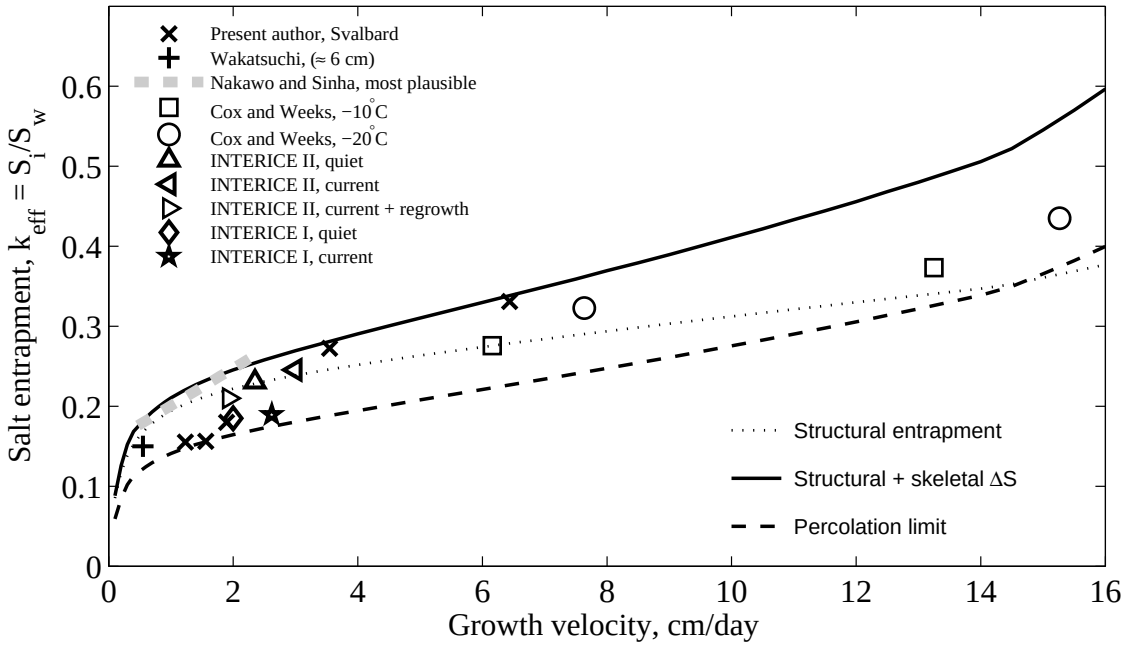

Figure 6: *Salt entrapment in sea ice. The reference data have been evaluated at ≈ 6 cm distance from the ice-water interface, based on (+) field data from Antarctic*[52]*, (x) present author's observations described in ref.*[21] *where also the INTERICE data are from several references are discussed (◇*[28]*; ⋆*[53]*; ◁ ▷ ▽△*[54]*). Due to unnatural growth conditions*[21]*, NaCl laboratory data from ref.*[24] *are only shown for $V > 3$ cm/day and $S_\infty < 40$. The grey dash-dotted line represents measured growth rates from ref.*[25]*. The curves are: The structural entrapment (thin dotted); the initial k_{sk} at the onset of bridging, where the structural value is augmented by the convectively limited salinity increase in the lower skeletal layer (solid upper curve); the lower bound 0.676 $\times k_{sk}$, based on the two-dimensional percolation conjecture (dashed curve). Observations fall consistently between upper and lower bounds.*

Henceforth a critical value of $d_{sk} = 0.10$ mm is used. The aforementioned conjecture is that the bridging process subsequently lowers the permeability and finally stabilises the salinity when a certain fraction of the brine layers is bridged. This fraction should be close to the theoretical threshold 0.676 from two-dimensional percolation theory, e. g.[31,51]. The simplistic approach limits the further salinity decrease to 0.676 of k_{sk} at the onset of bridging.

3 Sea ice salinity versus freezing rate

Equations (2) through (5) determine the relation between salt entrapment k_{eff} and growth velocity in dependence on seawater salinity. In figure 6 the predictions for $S_w = 35$ are compared to observations of k_{eff} for sea ice grown from normal seawater or NaCl solutions of comparable salinity. Observational data sets have been carefully evaluated 6 cm from the interface, a level above the highly unstable skeletal layer yet below the percolation limit (anticipated near a salinity minimum often found $\approx 10 - 15$ cm from the interface). The

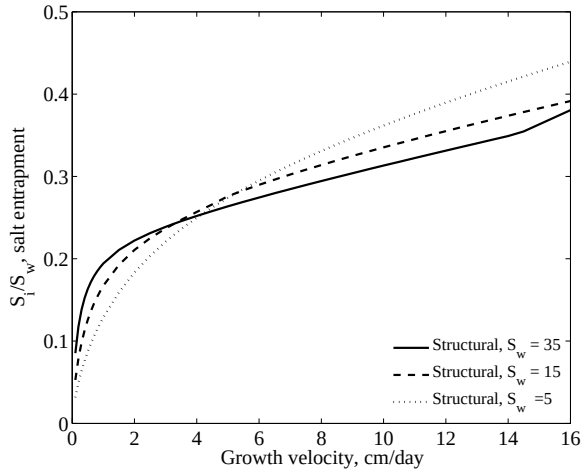

Figure 7: *Predicted structural salt entrapment* $(1 + \Delta S_{mi}/S_w)\ d_{sk}/a_0$ *for three seawater salinities.*

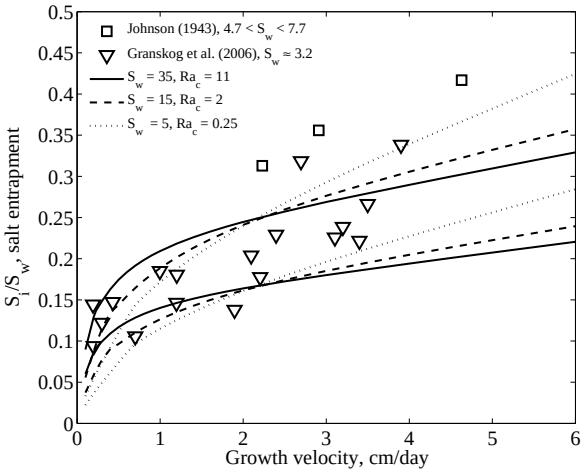

Figure 8: *Predicted upper* (k_{sk}*, onset of bridging) and lower bounds (0.676* k_{sk}*) for three salinities, compared to low salinity seawater observations*[56,29]*.*

available observations fall reasonably between the upper k_{sk} bound and $0.676 \times k_{sk}$, the lower percolation limit[c]. The variation of individual points is likely related to differences in under-ice currents and thermal history[21]. It is worth a note that the data from ref.[25], representing rapidly cooling ice with little thermal fluctuations, are consistently closest to the upper bound. The simple structural entrapment, disregarding the salinity increase ΔS_p in the skeletal layer, is also shown. It is nioted that at low growth velocity the dotted and solid curves merge, as the brine salinity gradient becomes very small.

The present approach also predicts how k_{eff} depends on seawater salinity. To illustrate the modelled behaviour, figure 7 compares the structural entrapment and interfacial supercooling $d_{sk}/a_0(1 + \Delta S_{mi}/S_w)$, excluding the internal salinity increase. At low growth velocities d_{sk}/a_0 implies an increase of k_{eff} with S_w, as a_0 increases with decreasing S_w (see figure 5). This effect is related to the boundary layer convection strength that begins to weaken at higher V for lower S_w, thus increasing a_0. The second factor, the interfacial $(1 + \Delta S_{mi}/S_w)$, becomes dominant at large growth velocities. With $\Delta S_{mi} \approx 1$ ‰ for all seawater salinities one finds an increase of k_{eff} with decreasing S_w.

The upper and lower bounds of the full prediction are shown in figure 8 for salinities 5, 15 and 35, along with observations of ice grown from low $S_w \approx 3.2$[29]. Note that the applied critical Rayleigh Numbers for $S_w = 35$ and 15 were determined empirically, while the value $Ra_{pc} = 0.25$ at $S_w = 5$ was chosen to match the observations in figure 8. The latter is, however, not unreasonable, as will be discussed in section 4 below. The effect of internal convection is to enhance the salinity dependence and steepen the slope in the relationship between k_{eff} and V at low seawater salinity. This is also consistent with limited earlier observations from Johnson[56]. His slightly larger k_{eff} is not unexpected, as his values are bulk salinities of 1 to 3 cm thick samples, likely including a more saline skeletal layer. The increasing k_{eff} with decreasing $S : w$ at high velocities is further supported by laboratory experiments from ref.[57] (not shown).

[c]Note that, while below $0.676 \times k_{sk}$ desalination driven by fluid flow is assumed negligible, some salinity decrease due to expansion upon freezing, e.g.[55], is still possible and likely enhanced by thermal cycling

Less agreement at lower growth velocities apparent in in figure 8 may be due to several factors. First, is the plate spacing expected to require a certain amount of ice growth, before adjusting to much larger values of a_0. Second, would a turbulent heat flux from the ocean to the ice require a larger effective temperature gradient for the same growth rate. This implies smaller plate spacing and larger k_{eff}, an effect suspected in laboratory data from ref.[35], see figure 5. Third, are ice growth rates uncertain: the lowest modelled growth rates shown in figure 8 are lower than the observed growth rates during that time (figure 3 of ref.[29]). Although not detailed enough for a validation, an earlier study of Baltic Sea ice by Palosuo[58] indicates $k_{eff} \approx 0.1$ for ice with $0.3 < V < 0.4$ cm d^{-1}, not inconsistent with the predictions in figure (8). To emphasise further validation the predicted $0.838k_{sk}$ between the bounds was, for the salinities $S_w = 35$ and 5, approximated by high-order polynomials[d].

4 Discussion

The proposed model for salt entrapment in sea ice provides further insight into the structure of the skeletal layer. The thickness of the latter has been determined by optical, mechanical and acoustical means to be rather stable between 2 and 4 centimeters (figure 9). The simulations of the Rayleigh-number-based convective layer thickness are compared in figure 10, with the solid curve for $S_w = 35$. Most noteworthy is that (i) the convecting layer thickness is considerably less than 2 to 4 cm and that (ii) it does not vary much over a wide range of growth rates. Comparing further the convecting layer thicknesses for the three salinities shows that ΔH_p increases with salinity.

To understand this behaviour it is helpful to compare two bounds. Consider first that the skeletal layer is given by some critical salinity excess ΔS_p. Assuming an average liquidus slope $\overline{m}$ this implies $\Delta H_p \sim \overline{m}\Delta S_p/(dT/dz)$, and as $V \sim dT/dz$ one would expect that ΔH_p decreases inversely with growth velocity. However, in reality equation (4) controls the stability, and replacing $\Delta S_p = \Delta H_p(dT/dz)/\overline{m}$ therein implies

$$\Delta H_p \sim (\overline{K} dT/dz)^{-1/2}. \tag{6}$$

With the permeability $\overline{K} \sim a_0^2$ increasing with growth velocity, (6) yields a quasi-constant convecting layer thickness under most natural growth conditions. As in reality $\overline{K}$ also depends on the near-interface porosity, and thus on the salt flux, one obtains the relationship in figure 10. Second, it is of interest to consider a salt-flux limit on the basis of a simple desalination constraint $\int_{t(z=0)}^{t(z=H_p)} (dS_i/dt)dt \approx S_w(k_{int} - k_{sk})$, where k_{int} is the value of k_{eff} at the interface. Assuming, as suggested by observations[24,55], desalination proportional to the temperature gradient and porosity, $dS_i/dt \sim \phi dT/dz$, and $dT/dz \sim V = dH/dt$ one obtains, neglecting a change in V for the small thickness change of interest,

$$\Delta H_{sk} \sim S_w \frac{(k_{int} - k_{sk})}{\overline{\phi}}. \tag{7}$$

[d]The curve for $S_w = 35$ was fitted for $0.1 < V < 16$ cm d^{-1} by the 9th order polynomial $k_{eff} = 0.0676 + 0.2161V - 0.1579V^2 + 6.618 \times 10^{-2}V^3 - 1.607 \times 10^{-2}V^4 + 2.368 \times 10^{-3}V^5 - 2.149 \times 10^{-4}V^6 + 1.172 \times 10^{-5}V^7 - 3.523 \times 10^{-7}V^8 + 4.486 \times 10^{-9}V^9$. For the restricted range $0.6 < V < 8$ cm d^{-1} a linear fit $k_{eff} = 0.144 + 0.03217V - 0.00166V^2$ represents the simulations within 5 %. At $S_w = 5$ a 7th order polynomial $k_{eff} = 0.00439 + 0.2338V - 0.1351V^2 + 5.077 \times 10^{-2}V^3 - 1.084 \times 10^{-2}V^4 + 1.304 \times 10^{-3}V^5 - 8.197 \times 10^{-5}V^6 + 2.095 \times 10^{-6}V^7$ is valid for $0.1 < V < 10$ cm d^{-1}, while in the restricted range $0.7 < V < 6$ cm d^{-1} a quadratic equation $k_{eff} = 0.0735 + 0.07295V - 0.00488V^2$ represents the simulations within 6 %.

In (7) $k_{int} \approx 1$, $k_{sk} \approx d_{sk}/a_0$ and the fraction on the right hand side is of order unity. One thus expects to first order $\Delta H_{sk} \sim S_w$ and a flux-limited skeletal layer that scales with the seawater salinity. In figure 10 a tentative bound $\Delta H_{sk} = S_w/10$ (suggested on the basis of observations for normal seawater) has been plotted three salinity values. The crossing of these bounds with the convection curves indicates where the convective layer prediction likely is not valid, because it reaches above the bridging regime, where the permeability is much smaller than given by equation 5. According to equation (6) this would increase ΔH_p even further. The system then probably cannot be described by the simplistic brine layer approach with harmonically averaged $\overline{K}$. For slowly growing ice the formation of brine channels, as observed in ref.[59], may be fundamental for the primary desalination.

A critical question is why the apparent critical Rayleigh Number for skeletal layer convection is so different for the three salinities. The sign shift of thermal expansion, taking for salinities < 24.7 place above the freezing point, stabilises the water thermally and has been suggested to play a role in this context[35]. However, its magnitude is rather small compared to the evolving haline density gradients. A more plausible explaination, pointed out in 'mushy layer' studies[60,37], appears to be the relative magnitude of the convecting skeletal layer ΔH_p compared to the interfacial boundary layer $\Delta H_c \approx 0.4 - 0.5$ mm. Simulations[60] indicate that the critical Rayleigh Number sharply decreases below a ratio of $H_p/H_c \approx 10$, a transition that in the present simulation is expected between $S_w = 35$ and 15. The rather low $Ra_{pc} = 0.25$, here employed to fit the salinity entrapment for $S_w = 5$, is not inconsistent with the latter simulations[60] and comparable values have been estimated indirectly in other systems as well[61]. A lower apparent Ra_{pc} would also be expected when convection takes place internal to single brine layers, and the effective permeability thus is ϕ^{-1} larger than given by equation 5. As discussed in ref.[21], larger grain sizes for lower S_w could then explain the observed behaviour. An important future goal is a determination of $Ra_{pc}(S_w)$ by theory and experiment, and in connection with observations of plate spacing and grain size.

5 Summary and outlook: geophysical modelling

A conceptual model for the entrapment of salt in sea ice has been formulated. The approach is based on simplistic convective stability models on both sides of the ice-water interface. Entrapment is controlled by two length-scales, the plate spacing a_0, depending on salinity and growth velocity, and the critical brine layer width at the onset of bridging between ice plates, assumed constant at $d_{sk} \approx 0.10$ mm. The plate spacing a_0 plays a fundamental role and couples the boundary layers. Being controlled by molecular diffusion and interface stability, its scaling is modified by compositional convection in a thin boundary layer in front of the advancing ice interface. It in turn controls the near-bottom permeability and extent of a lammelar high porosity skeletal layer. The implied dependence of salt entrapment on growth velocity and seawater salinity is consistent with most observations. However, open questions and uncertainties remain at very low growth velocities, where data are very sparse.

An important result of the model framework is the information obtained about the skeletal layer. Its rigorously convecting part of extent ΔH_p is predicted to be much smaller than its structural extent of $2 - 4$ cm. An indirect confirmation of convection, strong temperature fluctuations near the ice-water interface, indeed indicates a convecting layer thickness of a few millimeters[65,21]. Another aspect of interest in this connection are wider brine channels, known as locations of downward flow with a spacing of 1 to 5 cm in thin

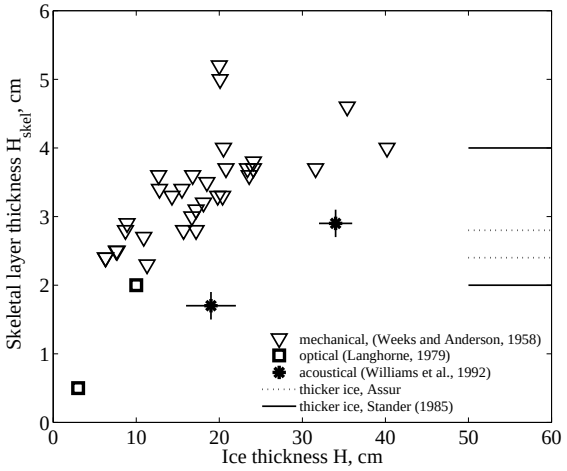

Figure 9: *Observations of the skeletal layer of young ice obtained by (i) mechanical scraping[62], (ii) visual inspection[63] and (iii) sound velocity measurements[64]. The dotted and solid lines span the range reported for thicker ice[62,45].*

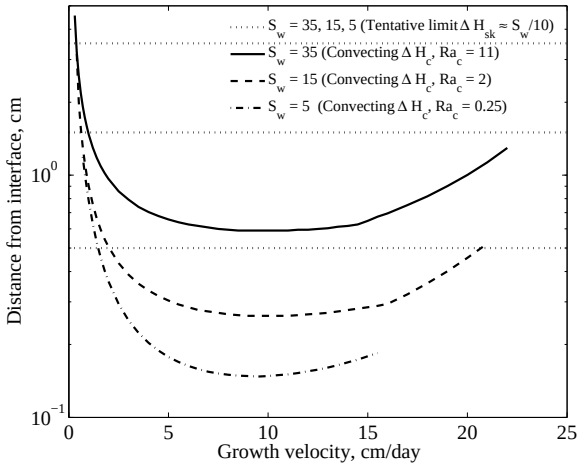

Figure 10: *Predicted convecting skeletal layer thickness ΔH_p near the sea ice interface for salinities 35, 15 and 5 assuming the indicated critical Rayleigh numbers. At high V instability does not occur; at low V the simulations were truncated when the bound $H_{sk} \approx S_w/10$ was exceeded.*

ice[48,66,44]. With expected normalised wave numbers of 1 to 2[60,37,41,42] similar cell spacings would follow from $\Delta H_p = 6 - 10$ mm, predicted for moderately growing sea ice. It thus appears likely that the spacing of brine channels is related to the identified mode of skeletal layer convection. If the analysis can be extended to the microstructure of Baltic Sea Ice, a thinner skeletal layer would imply more closely spaced but, likely, thinner brine channels. The present analysis indicates how structural observations and micro-modelling, lacking to date, might improve the predictability of its mechanical, optical and hydraulic properties.

Pore scales and skeletal layer extent can be expected to have direct implications for sea ice ecology[9,10] as well as dielectric sea ice properties relevant to remote sensing and radiative property modelling[11,67]. Another challenging problem in sea ice geophysics is to understand how the micro-scales influence meso-scale processes like fracturing, deformation, floe size formation, lead dynamics and rheology of sea ice fields on the large scale[6,68,69,70]. Here the role of micro scales is less clear. As an example, consider the critical stress intensity factor, or fracture toughness, which in terms of Griffith's theory, e.g.[71], may be written as $K_{Ic} = \sigma_t(2\pi c)^{1/2}$, where σ_t is the tensile strength and c the length of the controlling elliptic crack. With typical values obtained with small-scale sea ice specimen[71,72], $K_{Ic} \approx 0.11$ MPam$^{1/2}$ and $\sigma_t \approx 0.5$ MPa, one obtains a crack length of $c \approx 0.8$ cm. Inserting $K_{Ic} \approx 0.25$ MPam$^{1/2}$ obtained from larger scale field tests[72,70] gives $c \approx 4$ cm. The crack lengths thus compare to the skeletal layer scale, which emphasises the role of hydrodynamically controlled flaws and their possible impact on sea ice fracture processes. Moving to the geophysical scale, where $\sigma_t < 0.05$ MPa, then indicates that the strength of ice fields is rather controled by ice thickness and the length and depth of secondary thermal cracks[68,70]. It is a challenging question if and how these O(1-10)m cracks are in turn related to the hydrodynamically created flaws of order O($10^{-3} - 10^{-2}$)m. Another aspect where the skeletal layer might enter into mechanical problems is its influence on the friction coefficient of sea ice. The latter is relevant in modelling of ridging and rafting processes, e.g.[73,74], of which systematic

observations and concise theories are still incomplete. These considerations, and the different micro- and skeletal layer scales obtained here, emphasise to fill the gap in microstructure observations of Baltic Sea ice, also in order to understand its different strength behaviour compared to normal sea ice[15].

Another important aspect that follows from the present analysis is related to the permeability of sea ice and its variation in the near bottom fraction. In his analysis of sea ice properties Malmgren[16] once reported that sea ice at salinities of less than 5 ‰ kept a constant salt content for a rather long time, as long as the temperature remained below −4 to −5 °C. These properties correspond to a limiting brine porosity of 0.05 to 0.06. Since Malmgren's work several authors[75,76,50] have discussed this question in terms of different applications of percolation theory and proposed a critical porosity of $\phi_c \approx 0.05$. The present approach of the bridging transition employs, in contrast, a two-dimensional percolation concept. It is more realistic in terms of the microstructure[21] and implies that ϕ_c for young ice should be rather of order 0.676 d_{sk}/a_0, and thus in the range 0.1 to 0.15 for most natural growth conditions of sea ice. It also suggests that the critical porosity increases both with growth velocity and seawater salinity, as higher a_0 expected for Baltic Sea Ice implies a lower ϕ_c. It is emphasised that, while the present approach yields a threshold for (i) initial salt entrapment within cooling thin ice, Malmgren's critical porosity of 0.05 may be related to a different process, the (ii) desalination of old, warming winter ice that has undergone thermal cycling and subsequent microstructure metamorphosis. It is a future challenge to extend the present initial entrapment framework, and describe the desalination and microstructure of warming sea ice on the basis of a theory of this metamorphosis. To develop such a theory and further validate the present model concept, there is need for careful observations of microstructure and salinity under well-documented growth conditions.

References

[1] E. Drygalski, *Grönlands Eis und sein Vorland*, vol. 1 of *Grönland-Expedition der Gesellschaft für Erdkunde zu Berlin 1891-1893*, Berlin, Kühl, 1897, 555 pp.

[2] P. Hobbs, *Ice Physics*, Clarendon Press, Oxford, 1974, 837 pp.

[3] W. F. Weeks and S. F. Ackley, in *The Geophysics of Sea Ice*, vol. 146 of *NATO ASI Series*, Plenum Press, pp. 9–164, ed. by N. Untersteiner.

[4] V. F. Petrenko and R. W. Whitworth, *Physics of Ice*, Oxford University Press, 1999, 373 pp.

[5] B. Michel, *Ice Mechanics*, Les Presses De L'Université Laval, Québec, 1978, 499 pp.

[6] T. J. O. Sanderson, *Ice Mechanics - Risks to Offshore Structures*, Graham & Trotman, 1988, 253 pp.

[7] E. M. Schulson, *Eng. fracture mech.*, 2001, **68**, 1839.

[8] D. M. Cole, *Eng. fracture mech.*, 2001, **68**, 1797.

[9] I. A. Melnikov, *The Arctic Sea Ice Ecosystem*, Gordon and Breach, 1997, 204 pp.

[10] D. Thomas and G. S. Dieckmann, *Sea Ice: An Introduction to its Physics, Chemistry, Biology and Geology*, Blackwell, 2003, 402 pp.

[11] F. D. Carsey, *Microwave Remote Sensing of Sea Ice*, vol. 68 of *Geophysical Monograph*, American Geophysical Union, Washington, 1992.

[12] Y. P. Doronin and D. E. Kheisin, *Morskoi Led (Sea Ice)*, Gidrometeoizdat, Leningrad, 1975, english translation 1977 by Amerind Publishing, New Delhi, 318 pp.

[13] N. Untersteiner, *The Geophysics of Sea Ice*, vol. 146 of *NATO ASI Series, B: Physics*, Plenum Press, New York, 1986, 1196 pp.
[14] P. Wadhams, *Ice in the Ocean*, CRC Press, 2001, 351 pp.
[15] M. Leppäranta, *The Drift of Sea Ice*, Springer Praxis Books Geophysical Sciences, Springer, Berlin, 2005, 266 pp.
[16] F. Malmgren, *On the properties of sea ice*, vol. 1, No. 5 of *The Norwegian North Polar Expedition with the Maud 1918-1925, Scientific Results*, pp. 1–67, dissertation.
[17] G. F. N. Cox and W. F. Weeks, Salinity variations in sea ice, Research Report 310, U.S. Army Cold Regions Research and Engineering Laboratory, 1973.
[18] I. Melnikov, *J. Geophys. Res.*, 1995, **C3**, 4673.
[19] A. Y. Ryvlin, *Problems of the Arctic and Antarctic*, 1979, **45**, 99.
[20] A. Kovacs, Sea ice: Part I. Bulk salinity versus flow thickness, CRREL Report 96-7, U.S. Army Cold Regions Research and Engineering Laboratory, 1996.
[21] S. Maus, *On Brine Entrapment in Sea Ice: Morphological Stability, Microstructure and Convection*, Logos, Berlin, 2007, 538 pp.
[22] E. L. Moss, *Proc. Royal Soc. London*, 1878, **27**, 544.
[23] W. F. Weeks and G. Lofgren, in *Physics of Snow and Ice*, vol. 1, Hokkaido University, Sapporo, Japan, pp. 579–597.
[24] G. F. N. Cox and W. F. Weeks, Brine drainage and initial salt entrapment in sodium chloride ice, Research Report 345, U.S. Army Cold Regions Research and Engineering Laboratory, 1975, this research report consists of the dr.-philos. thesis *Brine drainage in sodium chloride ice* (1974) by G. F. N. Cox, Dartsmouth College, 179 pp.
[25] M. Nakawo and N. K. Sinha, *J. Glaciol.*, 1981, **27**, 315.
[26] R. Souchez, J. L. Tison and J. Jouzel, *Geophys. Res. Letters*, 1988, **15**, 1385.
[27] H. Eicken, *Deriving modes and rates of ice growth in the* W*eddell* S*ea from microstructural, salinity and stable-isotope data*, vol. 74 of *Antarctic Research Series*, pp. 89–122.
[28] H. Eicken, *From the microscopic to the macroscopic to the regional scale: growth, microstructure and properties of sea ice*, Blackwells Scientific Ltd., London, thomas, d. n. and dieckmann, g. s. (eds.) edn., pp. 22–81, 402 pp.
[29] M. A. Granskog, J. Uusikivi, A. Blanco Sequeiros and E. Sonninen, *Annals Glaciol.*, 2006, **44**, 134.
[30] J. A. Burton, R. C. Prim and W. P. Slichter, *J. Chem. Phys.*, 1953, **21**, 1987.
[31] D. Stauffer and A. Aharony, *Introduction to Percolation Theory*, Taylor & Francis, 2nd edition edn., 1992.
[32] W. W. Mullins and R. F. Sekerka, *J. Appl. Phys.*, 1964, **35**, 444.
[33] S. R. Coriell, G. B. MacFadden and R. F. Sekerka, *Ann. Rev. Mater. Sci.*, 1985, **15**, 119.
[34] S. Maus, *Prediction of the cellular microstructure of sea ice by morphological stability theory*, 11th Int. Conf. on Physics and Chemistry of Ice, Bremerhaven, Germany, Royal Society of Chemistry, pp. 371–382.
[35] G. Lofgren and W. F. Weeks, *J. Glaciol.*, 1969, **8**, 153.
[36] A. J. Gow, W. F. Weeks, P. Kosloff and S. Carsey, Petrographic and salinity characteristics of brackish water ice in the Bay of Bothnia, CRREL REPORT 92-13, Cold Regions Research and Engineering Laboratory, Hanover, 1992.
[37] M. G. Worster, *J. Fluid Mech.*, 1992, **237**, 649.
[38] M. G. Worster and J. S. Wettlaufer, *J. Phys. Chem. B*, 1997, **101**, 6132.
[39] D. A. Nield and A. Bejan, *Convection in Porous Media*, Springer, 2nd edn., 1999, 546

pp.
[40] R. McKibbin, *Transp. Por. Med.*, 1986, **1**, 271.
[41] K. E. Wilkes, *J. Heat Transfer ASME*, 1995, **117**, 543.
[42] D. A. Nield and A. Bejan, *Convection in Porous Media*, Springer, 3nd edn., 2006, 640 pp.
[43] D. A. Nield and C. T. Simmons, *Transp. Porous Med*, 2007, **68**, 413.
[44] J. S. Wettlaufer, M. G. Worster and H. E. Huppert, *J. Fluid Mech.*, 1997, **344**, 291.
[45] E. Stander, in *Int. Conf. on Port and Ocean Engineering*, vol. 1, Narssarssuaq, Greenland, pp. 168–176.
[46] D. L. Anderson and W. F. Weeks, *Trans. Amer. Geophys. Union*, 1958, **39**, 632.
[47] J. D. Harrison, *J. Appl. Phys.*, 1965, **36**, 326.
[48] T. M. Niedrauer and S. Martin, *J. Geophys. Res.*, 1979, **84**, 1176.
[49] V. L. Tsurikov, *Okeanologiia*, 1965, **5**, 463.
[50] C. Petrich, P. J. Langhorne and Z. F. Sun, *Cold Reg. Sci. Techn.*, 2006, **44**, 131.
[51] M. Sahimi, *Rev. of Mod. Phys.*, 1993, **65**, 1393.
[52] M. Wakatsuchi, *Low Temp. Sci.*, 1974, **A40**, 119.
[53] F. Cottier, H. Eicken and P. Wadhams, *J. Geophys. Res.*, 1999, **104**, 15859.
[54] J. Tison, C. Haas, M. M. Gowing, S. Sleewaegen and A. Bernard, *J. Glac.*, 2002, **48**, 177.
[55] G. F. N. Cox and W. F. Weeks, *J. Geophys. Res.*, 1988, **93**, 12449.
[56] J. G. Johnson, *Svenska hydrogr.-biolog. kommissionens skrifter, Ny serie: hydrografi*, 1943, **18**, 1.
[57] L. Fertuck, J. W. Spyker and W. H. Husband, *Can. J. Physics*, 1972, **50**, 264.
[58] E. Palosuo, *Havforskningsinstituttets Skrift*, 1963, **209**, 1.
[59] R. A. Lake and E. L. Lewis, *J. Geophys. Res.*, 1970, **75**, 583.
[60] F. Chen and C. F. Chen, *ASME J. Heat Transfer*, 1988, **110**, 403.
[61] C. Beckermann, J. P. Gu and W. J. Boettinger, *Metall. Mater. Trans. A*, 2000, **31 A**, 2545.
[62] W. F. Weeks and D. L. Anderson, *Trans. Amer. Geophys. Union*, 1958, **39**, 641.
[63] P. Langhorne, Crystal anisotropy in sea ice, Tech. rep., St. Johns, Newfoundland, Canada, 1979.
[64] K. L. Williams, G. R. Garrison and P. D. Mourad, *J. Acoust. Soc.Am.*, 1992, **92**, 2075.
[65] C. Haas, in J. G. K. U. Evers and A. van Os, eds., *Proceedings of the HYDROLAB workshop*, Hannover, Germany, pp. 107–113.
[66] M. Wakatsuchi and T. Saito, *Ann. Glaciol.*, 1985, **6**, 200.
[67] B. Light, G. A. Maykut and T. C. Grenfell, *J. Geophys. Res.*, 2004, **109**, C06013.
[68] J. Dempsey, The Johannes Weertman Symposium. The Minerals, Metals and Materials Society, pp. 351–361.
[69] J. Overland, B. A. Walter, T. B. Curtin and P. Turet, *J. Geophys. Res.*, 1995, 4559.
[70] J. P. Dempsey, *Int. J. Solids and Struct.*, 2000, **37**, 131.
[71] M. Mellor, in *The Geophysics of Sea Ice*, vol. 146 of *NATO ASI Series*, Plenum Press, pp. 165–281, ed. by N. Untersteiner.
[72] J. Dempsey, R. M. Adamson and S. V. Mulmule, *Int. J. Fracture*, 1999, **95**, 347.
[73] M. A. Hopkins and J. Tuhkuri, *J. Geophys. Res.*, 1999, **104**, 15815.
[74] J. Tuhkuri and M. Lensu, *J. Geophys. Res.*, 2002, **107**, 3125.
[75] K. M. Golden, S. F. Ackley and V. I. Lytle, *Science*, 1998, **282**, 2238.
[76] K. M. Golden, *Physica B*, 2003, **338**, 274.